The Thermodynamics of 3′-Terminal Pyrene and Guanosine for the Design of Isoenergetic 2′-*O*-Methyl-RNA-LNA Chimeric Oligonucleotide Probes of RNA Structure†

Anna Pasternak,‡,§ Elzbieta Kierzek,‡ Karol Pasternak,‡ Agata Fratczak,‡ Douglas H. Turner,|| and Ryszard Kierzek*,‡

Institute of Bioorganic Chemistry, Polish Academy of Sciences, 60-714 Poznan, Noskowskiego 12/14, Poland, and Department of Chemistry, University of Rochester, RC Box 270216, Rochester, New York 14627-0216

Received August 29, 2007; Revised Manuscript Received November 8, 2007

ABSTRACT: To facilitate design of short isoenergetic hybridization probes for RNA, we report the influence of adding 5′- or 3′-terminal 2′-*O*-methylguanosine (G^M), LNA-guanosine (G^L), or 3′-terminal pyrene pseudo-nucleotide (PPN) on the thermodynamic stability of 2′-*O*-methyl-RNA/RNA (2′-*O*-Me-RNA/RNA) duplexes with sequences 5′$C^MG^MG^MC^MA^M$/3′AAXGCCGUXAA, where X is A, C, G, or U. A 3′-terminal G^M or G^L added to the 2′-*O*-Me-RNA strand to form a G-A, G-G or G-U mismatch enhances thermodynamic stability ($\Delta\Delta G°_{37}$) of the 2′-*O*-Me-RNA/RNA duplexes on average by 0.7 and 1.5 kcal/mol, respectively. A 3′-terminal G^M or G^L in a G^M-C or G^L-C pair stabilizes the 2′-*O*-Me-RNA/RNA duplex by 2.6 and 3.4 kcal/mol, respectively. A 5′-terminal G^M or G^L in a G-A or G-G mismatch provided less stabilization in comparison with a 3′-terminal G-A or G-G mismatch, but more stabilization in a G-C or G-U pair. In contrast to guanosine derivatives, pyrene residue (P) as PPN at the 3′-terminal position enhances thermodynamic stability of the 2′-*O*-Me-RNA/RNA duplexes on average by 2.3 ± 0.1 kcal/mol, relatively independent of the type of ribonucleotide placed in the opposite strand. The thermodynamic data can be applied to design 2′-*O*-Me-RNA/RNA duplexes with enhanced thermodynamic stability that is also sequence independent. This is useful for design of hybridization probes to interrogate RNA structure and/or expression by microarray and other methods.

Knowledge about structure and interactions of RNA is crucial not only for understanding the biological functions of RNA but also for successfully targeting RNA with therapeutics (*1*−*3*). Prediction of RNA folding on the basis of free energy minimization is challenging (*4*, *5*). The influence on RNA thermodynamic stability of tertiary interactions, interactions of RNA with proteins and divalent cations, as well as RNA structural motifs such as pseudoknots and multibranch loops is not understood well (*6*, *7*). Enzymatic and chemical mapping of RNA provides a lot of detail about RNA structure, but can be time-consuming, although recent work by Weeks's group makes chemical mapping more rapid (*8*, *9*). Microarray approaches provide an even more rapid method for interrogating RNA structure. Southern and co-workers demonstrated the potential of this approach for studies of RNA structure (*10*−*12*). Microarrays based on short 2′-O-methylated heptanucleotide probes (non-isoenergetic microarrays) as well as LNA[1] (locked nucleic acids) modified 2′-O-methylated penta- and hexanucleotide probes (isoenergetic microarrays) can provide useful constraints for prediction of RNA secondary structures (*13*, *14*). In particular, hybridization to microarrays provides insight into unpaired nucleotides of target RNA.

RNAs with known secondary structures typically have short single stranded fragments, on average 3−7 nucleotides long. For that reason, short microarray probes are optimal to avoid disruption of target RNA secondary structure during hybridization. LNA modified 2′-O-methylated penta- and hexanucleotide probes are suitable for this application (*14*). In particular, incorporation of LNA and/or 2,6-diaminopurine nucleotides into probes is often enough for pentamers to provide at least the −6 kcal/mol in binding free energy at 37 °C ($\Delta G°_{37}$) required for detection (*14*−*16*). For regions where target RNA is A rich, however, it is necessary to enhance the thermodynamic stability. One approach is to add a 3′ G^L, which can pair with A, C, G, or U in the RNA target (Figure 1A) (*14*). The thermodynamic effects of such additions have not been previously studied, however.

† This work was supported by Polish State Committee for Scientific Research (2 PO4A 03729 to R.K. and N N301 3383 33 to E.K.) and NIH (GM22939 to D.H.T.).

* To whom correspondence should be addressed. E-mail: rkierzek@ibch.poznan.pl.

‡ Polish Academy of Sciences.

§ A.P. is a recipient of a fellowship from the President of the Polish Academy of Sciences.

|| University of Rochester.

[1] Abbreviations: PPN or P, pyrene pseudo-nucleotide; INA, intercalating nucleic acids; IPN, intercalating pseudo-nucleotide; LNA, locked nucleic acids; G^M, 2′-*O*-methylguanosine; G^L, LNA-guanosine; TLC, thin-layer chromatography; EDTA, ethylenediaminetetraacetate; NMR, nuclear magnetic resonance.

10.1021/bi701758z CCC: $40.75
Published on Web 01/05/2008

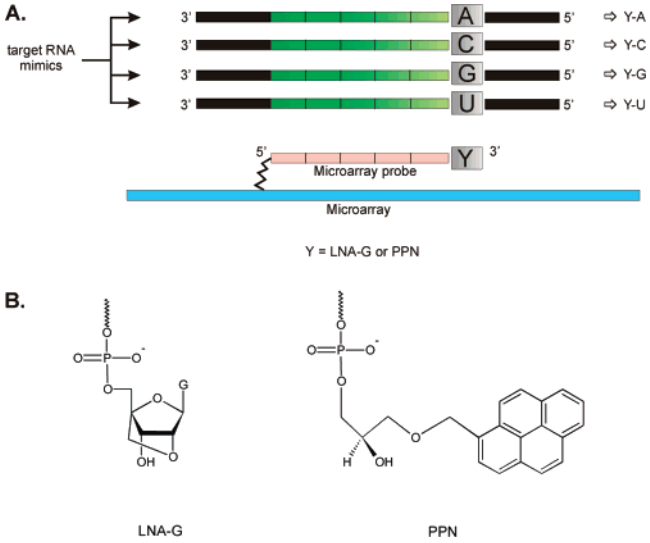

FIGURE 1: Origin of additional thermodynamic stabilization of hybridization duplexes. A. Scheme of interactions between target RNA mimics and microarray probe (red fragment is complementary to the green ones). B. Structures of LNA and PPN moiety placed at duplexes 3′-end.

This paper reports the influence of adding a 3′- or 5′-terminal 2′-*O*-methylguanosine or LNA-guanosine on the thermodynamic stability of RNA/2′-*O*-Me-RNA duplexes with sequence 5′AAXUGCCGXAA/3′$A^MC^MG^MG^MC^M$ where X is A, C, G, or U and superscript M denotes 2′-*O*-Me. When the 3′-terminal G is paired with U, A, or G, the duplex is stabilized on average by 0.7 ± 0.1 and 1.5 ± 0.2 kcal/mol for G^M and G^L, respectively. When the 3′-terminal G is paired with C, however, the duplex is stabilized by 2.6 and 3.4 kcal/mol for G^M and G^L, respectively. Even more sequence dependence is observed with a 5′-terminal G. This confounds design of a universal microarray in which relative binding depends only on the sequence of the first five nucleotides in a probe.

In principle, the sequence dependence of stability enhancement can be reduced by not employing hydrogen bonding interactions. In 2002, Pedersen's group developed the pyrene "intercalating pseudo-nucleotide" (IPN) which is the phosphoramidite of (*S*)-1-*O*-(4,4′-dimethoxytriphenylmethyl)-3-*O*-(1-pyrenylmethyl)glycerol. Incorporation of IPN into oligonucleotides resulted in formation of intercalating nucleic acids (INA) (*17*). Studies of the influence of IPN on thermodynamic stabilities of DNA/DNA, RNA/DNA and 2′-*O*-Me-RNA/DNA duplexes demonstrated that the pyrene derivative stabilizes DNA duplexes when it acts as a 5′-dangling end or as a bulge (*17*−*20*). When positioned as a dangling end, however, the stabilization may be due to stacking on the terminal base pair, rather than intercalation. Thus, we refer to the derivative as "pyrene pseudo-nucleotide" (PPN or P) (Figure 1B). Here we show that PPN at the 3′-end in 5′AAXUGCCGXAA/3′$PA^MC^MG^MG^MC^M$ duplexes enhances thermodynamic stability on average by 2.3 ± 0.1 kcal/mol, regardless of the type of ribonucleotide placed in the opposite strand. Thus it provides the characteristics required to design a microarray with probes that are universally isoenergetic for any target RNA. These characteristics should also be useful for designing isoenergetic microarrays for other purposes, including analysis of RNA expression.

EXPERIMENTAL PROCEDURES

General Methods. The 3′-*O*-phosphoramidites of LNA nucleotides were synthesized according to published procedures (*21*−*23*) with some minor modifications. TLC analysis of reaction progress was performed on Merck 60 F_{254} silica gel plates with various mixtures of dichloromethane and methanol (98:2 v/v, 95:5 v/v, 9:1 v/v and 8:2 v/v). Mass spectra of nucleosides and oligonucleotides were obtained on an LC MS Hewlett-Packard series 1100 MSD with API-ES detector or an MALDI TOF MS, model Autoflex (Bruker).

Synthesis and Purification of Oligonucleotides. Oligonucleotides were synthesized on an Applied Biosystems DNA/RNA synthesizer, using β-cyanoethyl phosphoramidite chemistry (*24*). Commercially available A, C, G, and U phosphoramidites with 2′-*O*-*tert*-butyldimethylsilyl or 2′-*O*-methyl groups were used for synthesis of RNA and 2′-*O*-methyl-RNA, respectively (Glen Research, Azco, Proligo). Thin-layer chromatography (TLC) purification of the oligonucleotides was carried out on Merck 60 F_{254} TLC plates with the mixture 1-propanol/aqueous ammonia/water = 55:35:10 (v/v/v). The details of deprotection and purification of oligoribonucleotides were described previously (*4*).

UV Melting. Oligonucleotide duplexes, in 10^{-3}−10^{-6} M concentration range, were melted in a buffer containing 100 mM sodium chloride, 20 mM sodium cacodylate, 0.5 mM Na_2EDTA, pH 7.0. The relatively low sodium chloride concentration kept melting temperatures in the reasonable range even when there were multiple substitutions, and also allowed comparison to previous experiments (*15*, *16*, *25*). Oligonucleotide single strand concentrations were calculated from absorbance above 80 °C with single strand extinction coefficients approximated by a nearest-neighbor model (*26*, *27*). Absorbance vs temperature melting curves were measured at 260 nm with a heating rate of 1 °C/min from 0 to 90 °C on a Beckman DU 640 spectrophotometer with a thermoprogrammer. Melting curves were analyzed and thermodynamic parameters were calculated from a two-state model with the program MeltWin 3.5 (*28*). For most duplexes, the $\Delta H°$ derived from T_M^{-1} vs $\ln(C_T/4)$ plots is within 15% of that derived from averaging the fits to individual melting curves (see Supporting Information), as expected if the two-state model is reasonable.

Fluorescence Measurements. Fluorescence was measured at room temperature with excitation at 340 nm and detection at 360−600 nm on a Perkin-Elmer LS 50B luminescence spectrometer using 500 μL quartz cells. All samples were prepared in buffer containing 100 mM sodium chloride, 20 mM sodium cacodylate, 0.5 mM Na_2EDTA, pH 7.0, with each strand at a concentration of 0.3 μM.

Chemical Synthesis of PPN Solid Support. The synthesis of PPN solid support was performed according to the procedures of previously reported synthesis of (*S*)-1-*O*-(4,4′-dimethoxytriphenylmethyl)-3-*O*-(1-pyrenylmethyl)glycerol (*17*) with expansion of the synthesis of immobilized PPN to solid support as described below (Figure 2).

*Succinic ester of 1-O-(4,4′-Dimethoxytriphenylmethyl)-3-O-(1-pyrenylmethyl)-glycerol (**2**).* 1-*O*-(4,4′-Dimethoxytriphenylmethyl)-3-*O*-(1-pyrenylmethyl)-glycerol (**1**) (280 mg, 0.46 mmol) was dissolved in 5 mL of dichloromethane and 55 mg (0.55 mmol) of succinic anhydride and 70 mg (0.55

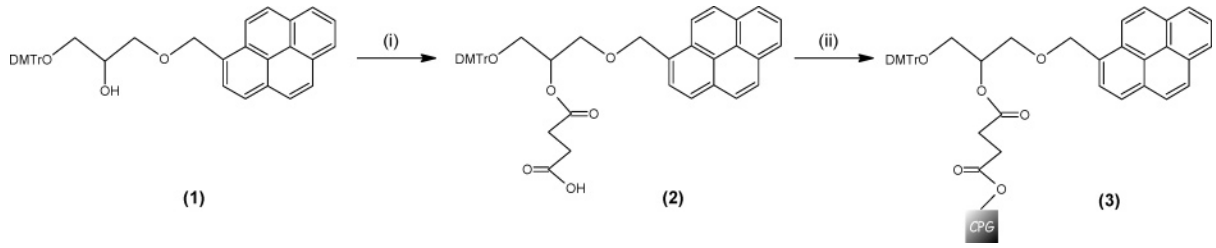

FIGURE 2: Chemical synthesis of PPN solid support. Reagents and conditions: (i) succinic anhydride, DMAP, CH_2Cl_2; (ii) 1. DMAP, DCC, amino lcaa CPG, DMF; 2. acetic anhydride, DMAP, pyridine.

mmol) of 4-dimethylaminopyridine were added. The reaction mixture was stirred at room temperature for 14 h. A saturated aqueous solution of sodium dihydrogen phosphate was added and extracted 3 times with dichloromethane. The organic layers were combined and washed 3 times with aqueous saturated solution of sodium bicarbonate. The organic phase was dried with anhydrous sodium sulfate and evaporated to give (**2**) as a white foam in quantitative yield. ^{1}H NMR ($CDCl_3$): δ 8.23−6.66 (m, 22H, $H_{arom.}$); 5.30 (m, 1H, H-4′); 5.22, 5.13 (2d, 2H, $-OCH_2-$ pyrenyl); 3.74 (d, 2H, H-5′); 3.23 (m, 2H, H-3′); 2.61 (s, 4H, $CH_2CH_2CO_2H$). ^{13}C NMR ($CDCl_3$): δ 171.96 (CO_2H); 158.36, 144.72, 136.70−123.41 ($C_{arom.}$, DMTr); 112.98 (DMTr); 85.94 ($OCPh_3$); 72.36 (C-3′); 71.69 ($-OCH_2-$ pyrenyl); 68.66 (C-2′); 55.08 ($2\times -CH_3$); 29.32, 29.20 ($CH_2CH_2CO_2H$). MALDI-MS *m/z*: 708.662 $[M + H]^+$ (calcd for $C_{45}H_{40}O_8$, 708.794).

*Solid Support of Succinic Ester of 1-O-(4,4′-Dimethoxytriphenylmethyl)-3-O-(1-pyrenylmethyl)-glycerol (**3**).* To the solution of succinic ester of 1-*O*-(4,4′-dimethoxytriphenylmethyl)-3-*O*-(1-pyrenylmethyl)-glycerol (**2**) (240 mg, 0.34 mmol) in dry DMF (5 mL) were added 43 mg (0.34 mmol) of 4-dimethylaminopyridine, 139 mg (0.67 mmol) of 1,3-dicyclohexylcarbodiimide (DCC) and 1.50 g of Native Amino lcaa CPG 500 Å. The mixture was gently shaken at room temperature for 24 h. The support was filtered and washed repeatedly with dichloromethane. Pyridine (7.5 mL), acetic anhydride (2.5 mL) and 4-dimethylaminopyridine (10 mg, 0.08 mmol) were added to the support. The mixture was left at room temperature for 1 h. The support was filtered again, washed repeatedly with dichloromethane, and dried. CPG loading: 47.9 μmol/g.

RESULTS

Chemical Synthesis of Modified Oligonucleotides. The published synthesis of protected LNA-guanosine phosphoramidite (*21*−*23*) was modified by replacing sodium benzoate by lithium benzoate in one of the synthetic steps and protecting the LNA-guanosine exocyclic amino group with *N*,*N*-dimethylaminomethylidene instead of an isobutyryl group. Preparation of PPN on solid support started with the published synthesis of (*S*)-1-*O*-(4,4′-dimethoxytriphenylmethyl)-3-*O*-(1-pyrenylmethyl)-glycerol (**1**) (*17*). Mixing of compound (**1**) and succinic anhydride in the presence of 4-dimethylaminopyridine gave derivative (**2**) in quantitative yield (Figure 2). Next, immobilization of compound (**2**) on solid support in the presence of 4-dimethylaminopyridine and DCC resulted in CPG loading by 47.9 μmol/g. Due to low steric hindrance of derivative (**2**), it was not necessary to prepare the active ester to load it on solid support. Oligonucleotides containing pyrene modifications were synthesized using standard β-cyanoethyl phosphoramidite chemistry (*24*).

The Influence of 5′-Terminal 2′-O-Methylguanosine and LNA-guanosine on the Thermodynamic Stability of 2′-O-Me-RNA/RNA Duplexes. The thermodynamic effect of a 5′-terminal G was measured with model duplexes, 5′G^M*C*^{M}*G*-^{M}*G*^{M}*C*^{M}*A*^{M}/3′AAX*GCCGU*XAA and 5′G^L*C*^{M}*G*^{M}*G*^{M}*C*^{M}*A*^{M}/3′AAX*GCCGU*XAA, where X is A, C, G or U and C^M, A^M, G^M are the respective 2′-*O*-methyl nucleotides, G^L is LNA-guanosine, and the italic fonts mark the Watson−Crick complementary regions within the duplexes (Table 1 and Figure 3b). The 2′-O-methylated oligonucleotides represent microarray probes and the oligoribonucleotides were longer to mimic RNA targets.

For the 5′-terminal G^M or G^L in a G-X base pair, the thermodynamic effect depends on X. For 5′G^M-G and 5′G^M-A, no effect was observed within experimental error (minor destabilization ($\Delta\Delta G°_{37}$) by 0.17 and 0.01 kcal/mol, respectively). In contrast, a 5′G^M-U or 5′G^M-C base pair stabilized duplexes by 1.68 and 4.63 kcal/mol, respectively. A 5′-terminal G^L-X base pair always improved duplex thermodynamic stability. The 5′G^L-G and 5′G^L-A pairs stabilized duplexes by 0.44 and 0.23 kcal/mol, respectively, while 5′G^L-U and 5′G^L-C pairs stabilized by 2.43 and 5.15 kcal/mol, respectively.

The Influence of 3′-Terminal 2′-O-Methylguanosine and LNA-guanosine on the Thermodynamic Stability of 2′-O-Me-RNA/RNA Duplexes. The thermodynamic effect of a 3′-terminal G^M-X or G^L-X base pair was measured with model duplexes, 5′*C*^{M}*G*^{M}*G*^{M}*C*^{M}*A*$^{M/L}$G^M/3′AAX*GCCGU*XAA and 5′*C*^{M}*G*^{M}*G*^{M}*C*^{M}*A*$^{M/L}$G^L/3′AAX*GCCGU*XAA, respectively (Figure 3c). When X was G, A, or U paired with G^M, the duplex was stabilized by 0.63, 0.65, and 0.85 kcal/mol, respectively, which are the same within experimental error (Table 1). In contrast, a 3′-terminal G^M-C base pair stabilized the duplex by 2.65 kcal/mol. Moreover, replacement of the 2′-*O*-methyladenosine within the 2′-*O*-Me-RNA/RNA duplex by LNA-adenosine caused additional stabilization ($\Delta\Delta G°_{37}$) by 1.15, 1.68, 0.83 and 1.64 kcal/mol for duplexes 3′-terminated with G^M-G, G^M-A, G^M-U, and G^M-C, respectively. That observation was in accordance with previously reported data concerning stabilization effects of LNA nucleotides (*15*).

The presence of an extra 3′-terminal G^L-X base pair increased thermodynamic stability of the duplex by 1.35, 1.63, 1.52 and 3.38 kcal/mol for X equal to G, A, U, or C, respectively. Substitution of 2′-*O*-methyladenosine 5′-adjacent to 3′-terminal G^L-X by LNA-adenosine caused additional stabilization of the duplex by 0.99, 1.10, 0.66 and 1.99 kcal/mol for duplexes terminated with 3′G^L-G, G^L-A, G^L-U and G^L-C, respectively.

The simultaneous influence of adding both 5′- and 3′-terminal 2′-*O*-methylguanosines on the thermodynamic stability of the 2′-*O*-Me-RNA/RNA duplexes was also

Table 1: Thermodynamic Parameters of Helix Formation between RNA and 2′-*O*-Me Oligoribonucleotides. The Effect of 2′-*O*-Methyl and LNA G-End[a]

RNA duplexes		T_M^{-1} vs log C_T plots					
RNA (5'-3')	2'-O-Me-RNA (5'-3')	$-\Delta H^o$ (kcal/mol)	$-\Delta S^o$ (eu)	$-\Delta G^o_{37}$ (kcal/mol)	T_M[b] (^oC)	$\Delta\Delta G^o_{37}$ (kcal/mol)	ΔT_M[b] (^oC)
AAG**UGCCG**GAA	$C^MG^MG^MC^MA^M$	58.5±4.8	165.1±15.6	7.34±0.13	41.4	0	0
5'G^M-G	$G^MC^MG^MG^MC^MA^M$	51.2±4.1	141.9±13.1	7.17±0.09	40.9	0.17	-0.5
3'G^M-G	$C^MG^MG^MC^MA^MG^M$	47.3±7.5	126.8±23.8	7.97±0.42	46.7	-0.63	5.3
3'G^M-G	$C^MG^MG^MC^M\underline{A^L}G^M$	47.0±1.7	122.2±5.3	9.12±0.08	55.1	-1.78	13.7
5' and 3' G^M-G	$G^MC^MG^MG^MC^MA^MG^M$	56.4±2.7	155.5±8.7	8.14±0.05	46.1	-0.80	4.7
5'$\underline{G^L}$-G	$\underline{G^L}C^MG^MG^MC^MA^M$	(36.6±2.2)	(93.0±7.0)	(7.78±0.07)	(48.0)	(-0.44)	(6.6)
3'$\underline{G^L}$-G	$C^MG^MG^MC^MA^M\underline{G^L}$	47.2±2.7	124.2±8.4	8.69±0.10	51.8	-1.35	10.4
3'$\underline{G^L}$-G	$C^MG^MG^MC^M\underline{A^LG^L}$	49.4±1.8	128.0±5.5	9.68±0.10	58.1	-2.34	16.7
AAA**UGCCG**AAA	$C^MG^MG^MC^MA^M$	48.6±7.8	133.0±25.4	7.32±0.39	42.1	0	0
5'G^M-A	$G^MC^MG^MG^MC^MA^M$	(32.5±1.4)	(81.4±4.5)	(7.31±0.03)	(44.6)	(0.01)	(2.5)
3'G^M-A	$C^MG^MG^MC^MA^MG^M$	46.5±4.2	124.3±13.3	7.97±0.16	46.9	-0.65	5.3
3'G^M-A	$C^MG^MG^MC^M\underline{A^L}G^M$	56.6±5.5	151.2±17.0	9.65±0.30	55.1	-2.33	13.0
5' and 3' G^M-A	$G^MC^MG^MG^MC^MA^MG^M$	43.8±1.8	115.5±5.7	7.95±0.03	47.4	-0.63	5.3
5'$\underline{G^L}$-A	$\underline{G^L}C^MG^MG^MC^MA^M$	34.2±3.2	86.0±10.3	7.55±0.13	46.6	-0.23	4.5
3'$\underline{G^L}$-A	$C^MG^MG^MC^MA^M\underline{G^L}$	50.6±3.7	134.2±11.6	8.95±0.16	52.6	-1.63	10.5
3'$\underline{G^L}$-A	$C^MG^MG^MC^M\underline{A^LG^L}$	52.8±4.0	137.9±12.0	10.05±0.25	59.1	-2.73	17.0
AAC**UGCCG**CAA	$C^MG^MG^MC^MA^M$	50.9±4.6	141.9±15.0	6.92±0.12	39.4	0	0
5'G^M-C	$G^MC^MG^MG^MC^MA^M$	67.4±17.3	180.0±52.3	11.55±1.16	62.0	-4.63	22.6
3'G^M-C	$C^MG^MG^MC^MA^MG^M$	62.3±0.7	170.0±2.2	9.57±0.03	52.9	-2.65	13.5
3'G^M-C	$C^MG^MG^MC^M\underline{A^L}G^M$	58.9±1.2	153.7±3.7	11.21±0.09	63.8	-4.29	24.4
5' and 3' G^M-C	$G^MC^MG^MG^MC^MA^MG^M$	61.0±2.8	155.5±8.4	12.80±0.21	72.5	-5.88	33.1
5'$\underline{G^L}$-C	$\underline{G^L}C^MG^MG^MC^MA^M$	57.6±2.3	146.7±6.9	12.07±0.20	70.0	-5.15	30.6
3'$\underline{G^L}$-C	$C^MG^MG^MC^MA^M\underline{G^L}$	52.1±4.3	134.7±13.1	10.30±0.28	61.2	-3.38	21.8
3'$\underline{G^L}$-C	$C^MG^MG^MC^M\underline{A^LG^L}$	65.3±3.4	170.8±10.2	12.29±0.28	67.0	-5.37	27.6
AAU**UGCCG**UAA	$C^MG^MG^MC^MA^M$	46.5±3.9	127.3±12.6	7.07±0.12	40.6	0	0
5'G^M-U	$G^MC^MG^MG^MC^MA^M$	51.5±3.7	137.7±11.6	8.75±0.14	51.0	-1.68	10.4
3'G^M-U	$C^MG^MG^MC^MA^MG^M$	54.8±4.8	151.3±15.5	7.92±0.15	45.1	-0.85	4.5
3'G^M-U	$C^MG^MG^MC^M\underline{A^L}G^M$	42.3±1.6	108.1±5.0	8.75±0.07	54.2	-1.68	13.6
5' and 3' G^M-U	$G^MC^MG^MG^MC^MA^MG^M$	63.6±3.3	173.1±10.3	9.89±0.13	54.3	-2.82	13.7
5'$\underline{G^L}$-U	$\underline{G^L}C^MG^MG^MC^MA^M$	53.4±0.8	141.5±2.6	9.50±0.04	55.3	-2.43	4.3
3'$\underline{G^L}$-U	$C^MG^MG^MC^MA^M\underline{G^L}$	52.2±1.4	140.5±4.3	8.59±0.03	49.7	-1.52	4.6
3'$\underline{G^L}$-U	$C^MG^MG^MC^M\underline{A^LG^L}$	44.1±1.9	112.4±5.7	9.25±0.09	57.4	-2.18	16.8

[a] Solutions are 100 mM sodium chloride, 20 mM sodium cacodylate, and 0.5 mM Na_2EDTA, pH 7. Values in parentheses are from non-two-state melts. [b] Calculated for 10^{-4} M oligomer concentration.

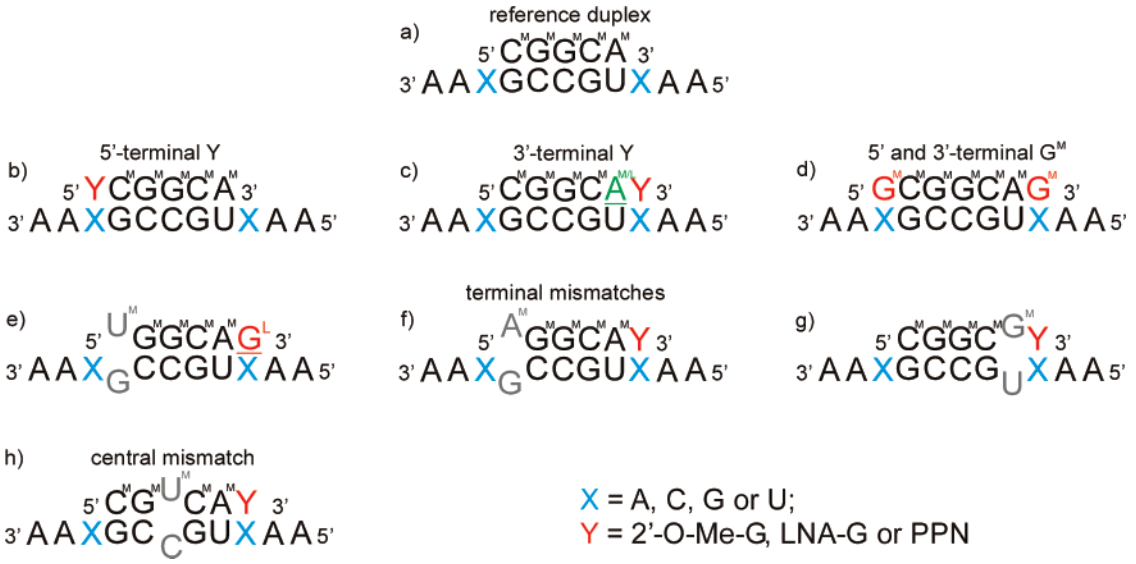

FIGURE 3: Structures of various 2′-*O*-Me-RNA/RNA duplexes used during the studies.

investigated. The duplexes were stabilized by 0.80, 0.63, 2.82, and 5.88 kcal/mol for G^M-X pairs when X was G, A, U or C, respectively (Table 1 and Figure 3d). The values are within experimental error of the sum of the measured effects for the separated 5′- or 3′-terminal G^M-X base pairs.

The Influence of Mismatches on Thermodynamic Stability of 2′-O-Me-RNA/RNA Duplexes with a 3′-Terminal LNA-guanosine. The influence of mismatches was studied for two 2′-*O*-Me-RNA/RNA duplexes, which differed in a G^L-G or G^L-C base pair at the 3′-end (Table 2 and Figure 3e−h). The single mismatches were placed at the 5′-terminal and central position as well as adjacent to the 3′-terminal G^L-X pair in the probe strand. The 5′-terminal U^M-G mismatch (Figure 3e) decreased thermodynamic stability by 1.07 and 0.51 kcal/mol for 2′-*O*-Me-RNA/RNA duplexes containing 3′-terminal G^L-G and G^L-C base pairs, respectively. An A^M-G mismatch at the 5′-terminal position (Figure 3f) reduced thermodynamic stability by 0.88 kcal/mol for the duplex with a 3′-terminal G^L-G base pair and had no significant effect ($\Delta\Delta G°_{37} = -0.06$ kcal/mol) with the 3′G^L-C base pair. When the G^M-U mismatch was adjacent to the 3′-terminal G^L-X base pair (Figure 3g), destabilization ($\Delta\Delta G°_{37}$) was 0.52 and 0.91 kcal/mol for 3′G^L-G and 3′G^L-C, respectively. Finally, the centrally placed U^M-C (Figure 3h) mismatch caused significant destabilization by 1.68 and 4.68 kcal/mol for 3′G^L-G and 3′G^L-C base pairs, respectively.

The Influence of PPN Placed at the 3′-End on Thermodynamic Stability of 2′-O-Me-RNA/RNA Duplexes. The thermodynamic studies of the influence of a 3′-terminal pyrene residue were carried out with the model duplex, 5′$C^MG^MG^MC^MA^M$P/3′AAX*GCCGU*XAA, where P is the pyrene derivative (Figure 3c with Y = P). The 3′-terminal pyrene enhanced duplex stability by 2.17, 2.22, 2.36 and 2.43 kcal/mol when X was G, A, C or U, respectively (Table 3). Thus the enhancement is independent of X within experimental error. Furthermore, substitution of the 2′-*O*-methyladenosine by LNA-adenosine caused additional stabilization by 1.58, 1.45, 1.10 and 1.36 kcal/mol for X equal to G, A, C or U, respectively.

The Influence of Mismatches on Thermodynamic Stability of 2′-O-Me-RNA/RNA Duplexes with a 3′-Terminal PPN. The influence of mismatches was studied for two 2′-*O*-Me-RNA/RNA duplexes, which differed in positioning a 3′-terminal PPN opposite to G or C in the oligoribonucleotide strand (Table 4 and Figure 3f, g, and h). Similarly to previous experiments, the single mismatches were placed at 5′-terminal and central positions as well as adjacent to the 3′-terminal PPN within the model 2′-*O*-Me-RNA/RNA duplexes.

The A^M-G mismatch placed at the 5′-terminal position destabilized 2′-*O*-Me-RNA/RNA duplexes containing PPN by 1.01 kcal/mol for the duplex with PPN opposite to G (3′P-G), and by 0.78 kcal/mol for the duplex with PPN opposite to C (3′P-C). Similar effects were observed when a G^M-U mismatch was adjacent to the 3′P-X ($\Delta\Delta G°_{37}$ = 0.80 kcal/mol for 3′P-G and 0.79 kcal/mol for 3′P-C). Finally, a centrally positioned U^M-C mismatch caused the largest destabilization, 2.21 and 3.15 kcal/mol for 3′P-G and 3′P-C, respectively.

Fluorescence of PPN. Figure 4 shows fluorescence spectra of single stranded, 5′$C^MG^MG^MC^MA^M$P and duplexes, 5′$C^MG^MG^MC^MA^M$P/3′AAX*GCCGU*XAA at 0.3 μM of each strand. There is a 3- to 4-fold reduction of fluorescence at 378 and 398 nm, regardless of type of nucleotide in the RNA strand. Thus fluorescence intensity could be used to monitor hybridization.

DISCUSSION

Oligonucleotide probes can provide insights into RNA structure. For example, isoenergetic oligonucleotide microarrays provide a rapid method to study the secondary structure and interactions of folded RNA (*14*). Single stranded regions of RNA are mostly 3−7 nucleotides long. Thus, isoenergetic pentanucleotides are well suited for revealing these regions. Interpretation of the data is simplified if the thermodynamic stability of the hybridization duplex formed by single stranded fragments and the Watson−Crick complementary probes is independent of sequence so that the only factor determining the detectable hybridization is the competition with the folded structure of the target RNA. It is difficult, however, to design probes to provide equal duplex stabilities for GC rich and AU rich sequences. Here, thermodynamics

Table 2: Thermodynamic Parameters of Helix Formation with RNA and 2′-*O*-Me Oligoribonucleotides. The Effect of Mismatches and LNA G 3′-End[a]

RNA duplexes		T_M^{-1} vs log C_T plots							
RNA (5'-3')	2'-O-Me-RNA (5'-3')	$-\Delta H^o$ (kcal/mol)	$-\Delta S^o$ (eu)	$-\Delta G^o_{37}$ (kcal/mol)	T_M[b] (^{o}C)	$\Delta\Delta G^o_{37}$ (kcal/mol)	ΔT_M[b] (^{0}C)	$\Delta\Delta G^o_{37}$ (kcal/mol)	ΔT_M[b] (^{o}C)
AAG**UGCCG**GAA	$C^MG^MG^MC^MA^M$	58.5±4.8	165.1±15.6	7.34±0.13	41.4	0	0		
3'$\underline{G^L}$-G	$C^MG^MG^MC^MA^M\underline{G^L}$	47.2±2.7	124.2±8.4	8.69±0.10	51.8			0	0
G^M-U	$C^MG^MG^MC^MG^M$	42.7±1.8	113.2±5.6	7.60±0.03	45.0	-0.26	3.6		
3'$\underline{G^L}$-G / G^M-U	$C^MG^MG^MC^MG^M\underline{G^L}$	42.9±0.7	112.0±2.2	8.17±0.02	49.3			0.52	-2.5
U^M-G	$U^MG^MG^MC^MA^M$	42.5±2.2	114.8±7.3	6.91±0.05	39.8	0.43	-1.6		
3'$\underline{G^L}$-G / U^M-G	$U^MG^MG^MC^MA^M\underline{G^L}$	41.3±1.2	108.7±3.8	7.62±0.02	45.4			1.07	-6.4
A^M-G	$A^MG^MG^MC^MA^M$	38.4±1.8	101.0±5.8	7.02±0.04	41.0	0.32	-0.4		
3'$\underline{G^L}$-G /A^M-G	$A^MG^MG^MC^MA^M\underline{G^L}$	44.8±1.1	119.3±3.4	7.81±0.01	46.1			0.88	-5.7
U^M-C	$C^MG^MU^MC^MA^M$	44.1±1.1	119.9±3.7	6.91±0.02	39.7	0.43	-1.7		
3'$\underline{G^L}$-G /U^M-C	$C^MG^MU^MC^MA^M\underline{G^L}$	35.6±1.7	92.3±5.5	7.01±0.04	41.2			1.68	-10.6
AAC**UGCCG**CAA	$C^MG^MG^MC^MA^M$	50.9±4.6	141.9±15.0	6.92±0.12	39.4	0	0		
3'$\underline{G^L}$-C	$C^MG^MG^MC^MA^M\underline{G^L}$	52.1±4.3	134.7±13.1	10.30±0.28	61.2			0	0
G^M-U	$C^MG^MG^MC^MG^M$	(30.3±2.0)	(75.2±6.4)	(6.97±0.07)	(41.6)	(-0.05)	(2.2)		
3'$\underline{G^L}$-C / G^M-U	$C^MG^MG^MC^MG^M\underline{G^L}$	53.1±1.9	141.0±5.8	9.39±0.07	54.6			0.91	-6.6
U^M-G	$U^MG^MG^MC^MA^M$	(34.3±1.8)	(89.5±5.8)	(6.49±0.06)	(36.7)	(0.43)	(-2.7)		
3'$\underline{G^L}$-C / U^M-G	$U^MG^MG^MC^MA^M\underline{G^L}$	54.9±1.6	145.4±5.0	9.79±0.08	56.6			0.51	-4.6
A^M-G	$A^MG^MG^MC^MA^M$	36.1±1.1	94.8±3.6	6.68±0.02	38.6	0.24	-0.8		
3'$\underline{G^L}$-C /A^M-G	$A^MG^MG^MC^MA^M\underline{G^L}$	59.5±1.1	158.4±3.4	10.36±0.06	58.4			-0.06	-2.8
U^M-C	$C^MG^MU^MC^MA^M$	45.7±1.8	128.7±6.0	5.81±0.06	32.2	1.11	-7.2		
3'$\underline{G^L}$-C /U^M-C	$C^MG^MU^MC^MA^M\underline{G^L}$	47.1±3.1	133.9±10.3	5.62±0.12	31.1			4.68	-30.1

[a] Solutions are 100 mM sodium chloride, 20 mM sodium cacodylate, and 0.5 mM Na_2EDTA, pH 7. Values in parentheses are from non-two-state melts. [b] Calculated for 10^{-4} M oligomer concentration.

are presented that provide two solutions to this problem. One solution is to add a 3′-terminal G^L to the pentamer sequence. The second solution is to add a 3′-terminal PPN (Figure 1A).

Previous studies have provided thermodynamic increments for many terminal mismatches in RNA/RNA duplexes (*29*−*32*). These data show that a 3′-terminal G provides roughly the same stability increment when paired with A, G, or U, but a more favorable increment when paired with C. In contrast, a 5′-terminal G provides roughly the same stability increment when paired with A or G, but a more favorable increment when paired with U, and the most favorable increment when paired with C. This suggested that a 3′-terminal G would provide a more sequence independent probe than a 5′-terminal G. Another advantage of adding additional stability at the 3′-end of the probe is that dangling end stacking from the target RNA is changed at the 5′-end, and 5′-dangling end stacking is relatively independent of sequence (*32*). In contrast, adding a 5′-terminal G to the probe changes the dangling end at the 3′-side of the target RNA, and 3′-dangling end stacking is very sequence dependent (*32*).

The expectations described above are largely observed in the 2′-*O*-Me-RNA/RNA duplexes with either a terminal G^M or G^L as listed in Table 1. Terminal G-A, G-G, or G-U mismatches containing 3′G^M and 3′G^L (Figure 3c) enhanced the thermodynamic stability of 2′-*O*-Me-RNA/RNA duplexes on average by 0.7 ± 0.1 and 1.5 ± 0.2 kcal/mol, respectively, at 37 °C. The 0.7 kcal/mol is identical to the average predicted for RNA/RNA duplexes at 1 M NaCl when the terminal sequence is 5′AG/3′UX (*32*). On the basis of free energy parameters for RNA/RNA duplexes (*32*), the free energy enhancement for terminal 3′G^M mismatches will depend on the preceding base pair, reaching a maximum of about 1.5 kcal/mol at 37 °C when the preceding base pair is CG. Additional substitution by LNA-adenosine for the 2′-*O*-methyladenosine adjacent to the 3′-terminal G^L-X base pairs within the 2′-*O*-Me-RNA/RNA duplexes studied here

Table 3: Thermodynamic Parameters of Helix Formation with RNA and 2′-*O*-Me Oligoribonucleotides.The Effect of PPN (P) 3′-End[a]

RNA duplexes		T_M^{-1} vs log C_T plots					
RNA (5'-3')	2'-O-Me-RNA (5'-3')	$-\Delta H^o$ (kcal/mol)	$-\Delta S^o$ (eu)	$-\Delta G^o_{37}$ (kcal/mol)	T_M[b] (^oC)	$\Delta\Delta G^o_{37}$ (kcal/mol)	ΔT_M[b] (^oC)
AAG**UGCCG**GAA	$C^MG^MG^MC^MA^M$	58.5±4.8	165.1±15.6	7.34±0.13	41.4	0	0
3'**P**-G	$C^MG^MG^MC^MA^M$**P**	50.2±2.6	131.2±8.0	9.51±0.12	56.6	-2.17	15.2
3'**P**-G	$C^MG^MG^MC^M$**A**^{L}**P**	59.3±1.3	155.6±4.0	11.09±0.08	62.8	-3.75	21.4
AAA**UGCCG**AAA	$C^MG^MG^MC^MA^M$	48.6±7.8	133.0±25.4	7.32±0.39	42.1	0	0
3'**P**-A	$C^MG^MG^MC^MA^M$**P**	50.2±1.1	131.1±3.5	9.54±0.05	56.8	-2.22	14.7
3'**P**-A	$C^MG^MG^MC^M$**A**^{L}**P**	57.0±1.4	148.5±4.1	10.99±0.09	63.3	-3.67	21.2
AAC**UGCCG**CAA	$C^MG^MG^MC^MA^M$	50.9±4.6	141.9±15.0	6.92±0.12	39.4	0	0
3'**P**-C	$C^MG^MG^MC^MA^M$**P**	50.9±3.2	134.2±9.9	9.28±0.15	54.7	-2.36	15.3
3'**P**-C	$C^MG^MG^MC^M$**A**^{L}**P**	51.8±1.4	133.4±4.2	10.38±0.09	61.9	-3.46	22.5
AAU**UGCCG**UAA	$C^MG^MG^MC^MA^M$	46.5±3.9	127.3±12.6	7.07±0.12	40.6	0	0
3'**P**-U	$C^MG^MG^MC^MA^M$**P**	52.7±2.6	139.3±8.1	9.50±0.10	55.5	-2.43	14.9
3'**P**-U	$C^MG^MG^MC^M$**A**^{L}**P**	56.3±1.1	146.4±3.3	10.86±0.06	62.8	-3.79	22.2

[a] Solutions are 100 mM sodium chloride, 20 mM sodium cacodylate, and 0.5 mM Na_2EDTA, pH 7. [b] Calculated for 10^{-4} M oligomer concentration.

caused further stabilization, on average by 0.9 kcal/mol at 37 °C. When the 5′-terminal $G^{M/L}$ paired with C, the stability enhancement was much larger, 2.65 and 3.38 kcal/mol for G^M and G^L, respectively (Table 2 and Figure 5). This is somewhat larger than the values of 1.8 and 3.0 kcal/mol predicted on the basis of nearest neighbor parameters for Watson−Crick pairs (*25*) and the effect of a 3′LNA (*15*). The added GC pair also changes the 5′ dangling end from a C on a U to an A on a C, which can account for 0.4 kcal/mol of the difference between measured and predicted values (*32*).

As expected, the influence of 5′-terminal $G^{M/L}$-X base pairs (Figure 3b) on the thermodynamic stability of 2′-*O*-Me-RNA/RNA duplexes was more complex than the 3′-terminal ones. Interaction of an additional 2′-*O*-methylguanosine or LNA-guanosine with A or G in the opposite RNA strand gave only minor duplex stabilization with G^L and essentially no effect with G^M ($\Delta\Delta G^\circ_{37} = 0.17$ and 0.01 kcal/mol for G^M-G and G^M-A, respectively). The lack of stabilization by G^M may reflect changes in 3′-dangling end stacking in the duplex. On the other hand, the interactions of both G^M and G^L with pyrimidines gave significant stabilization ($\Delta\Delta G^\circ_{37} = -4.63$, -5.15, -1.68 and -2.43 kcal/mol for 5′G^M-C, G^L-C, G^M-U and G^L-U, respectively). For RNA/RNA duplexes (*32*), $\Delta\Delta G^\circ_{37}$ is predicted to be -4.7 ($= -3.4 - 1.7 + 0.4$) kcal/mol when one terminus changes from $^{5'GC3'}_{C}$ to $^{5'GCA3'}_{CG}$. This is essentially identical to the measured value of -4.6 kcal/mol for the addition of the 5′G^M-C base pair, where the 3′-dangling end changes from a C on a G (-0.4 kcal/mol) to an A on a C (-1.7 kcal/mol). Assuming that 3′-dangling end stacking on a UG pair is identical to that on a UA pair, a similar calculation for one terminus changing from $^{5'GU3'}_{C}$ to $^{5'GUA3'}_{CG}$ predicts $\Delta\Delta G^\circ_{37} = -2.6$ ($=-2.5 - 0.7 + 0.6$) kcal/mol, somewhat more favorable than the -1.7 kcal/mol measured for addition of the 5′G^M-U base pair.

Stabilization was also observed when additional 2′-*O*-methylguanosines were present at both the 5′- and 3′-terminal positions within the 2′-*O*-Me-RNA/RNA duplexes (Figure 3d). Within experimental error, the effects of the two ends were roughly additive.

When single mismatches U^M-C, U^M-G, G^M-U and A^M-G were present at various positions within the 2′-*O*-Me-RNA/RNA duplexes containing 3′-terminal G^L-G or G^L-C base pairs, significant destabilization was mostly observed (Table 2). The destabilization was largest when the mismatch was in the center of the duplex (Figure 3h). For example, a U^M-C mismatch positioned in the center of a duplex made thermodynamic stability ($\Delta\Delta G^\circ_{37}$) less favorable by 1.68 and 4.68 kcal/mol, respectively, for the duplexes containing an additional 3′-terminal G^L-G or G^L-C base pair. This is a non-nearest neighbor effect because the effect of a mismatch depends on the number of Watson−Crick base pairs. The placement of mismatches at the 5′-terminus (U^M-G and A^M-G as in Figures 3e and 3f, respectively) or at the position adjacent (G^M-U) to 3′-terminal G^L-G or G^L-C (Figure 3g) destabilized the duplexes much less. Generally, the observations concerning the positional influence of mismatches within the duplex on thermodynamic stability are consistent with previously reported data (*15*). Interestingly, destabilization by single U^M-C, U^M-G, G^M-U and A^M-G mismatches was usually larger when an additional 3′G^L-G or 3′G^L-C base pair was present. For example, a 5′-terminal U^M-G mismatch in the 2′-*O*-Me-RNA/RNA duplex containing a 3′-terminal G^L-G (Figure 3e) decreased thermodynamic stability by 1.07

Table 4: Thermodynamic Parameters of Helix Formation with RNA and 2′-*O*-Me Oligoribonucleotides. The Effect of Mismatches and PPN (P) 3′-End[a]

RNA duplexes		T_M^{-1} vs log C_T plots							
RNA (5'-3')	2'-O-Me-RNA (5'-3')	-ΔH° (kcal/mol)	-ΔS° (eu)	$-\Delta G^\circ_{37}$ (kcal/mol)	T_M[b] (°C)	$\Delta\Delta G^\circ_{37}$ (kcal/mol)	ΔT_M[b] (°C)	$\Delta\Delta G^\circ_{37}$ (kcal/mol)	ΔT_M[b] (°C)
AAG**UGCCG**GAA	$C^MG^MG^MC^MA^M$	58.5±4.8	165.1±15.6	7.34±0.13	41.4	0	0		
3'**P**-G	$C^MG^MG^MC^MA^M$**P**	50.2±2.6	131.2±8.0	9.51±0.12	56.6			0	0
G^M-U	$C^MG^MG^MC^MG^M$	42.7±1.8	113.2±5.6	7.60±0.03	45.0	-0.26	3.6		
3'**P**-G/G^M-U	$C^MG^MG^MC^MG^M$**P**	45.2±1.3	117.7±4.1	8.71±0.04	52.7			0.80	-3.9
A^M-G	$A^MG^MG^MC^MA^M$	38.4±1.8	101.0±5.8	7.02±0.04	41.0	0.32	-0.4		
3'**P**-G/A^M-G	$A^MG^MG^MC^MA^M$**P**	48.4±1.1	128.6±3.3	8.50±0.03	50.1			1.01	-6.5
U^M-C	$C^MG^MU^MC^MA^M$	44.1±1.1	119.9±3.7	6.91±0.02	39.7	0.43	-1.7		
3'**P**-G/U^M-C	$C^MG^MU^MC^MA^M$**P**	47.0±1.8	128.0±5.7	7.30±0.03	42.1			2.21	-14.5
AAC**UGCCG**CAA	$C^MG^MG^MC^MA^M$	50.9±4.6	141.9±15.0	6.92±0.12	39.4	0	0		
3'**P**-C	$C^MG^MG^MC^MA^M$**P**	50.9±3.2	134.2±9.9	9.28±0.15	54.7			0	0
G^M-U	$C^MG^MG^MC^MG^M$	(30.3±2.0)	(75.2±6.4)	(6.97±0.07)	(41.6)	(-0.05)	(2.2)		
3'**P**-C/G^M-U	$C^MG^MG^MC^MG^M$**P**	41.7±1.0	107.1±3.0	8.49±0.03	52.3			0.79	-2.4
A^M-G	$A^MG^MG^MC^MA^M$	36.1±1.1	94.8±3.6	6.68±0.02	38.6	0.24	-0.8		
3'**P**-C/A^M-G	$A^MG^MG^MC^MA^M$**P**	45.4±0.5	118.9±1.5	8.50±0.02	51.0			0.78	-3.7
U^M-C	$C^MG^MU^MC^MA^M$	45.7±1.8	128.7±6.0	5.81±0.06	32.2	1.11	-7.2		
3'**P**-C/U^M-C	$C^MG^MU^MC^MA^M$**P**	45.8±2.1	128.0±7.0	6.13±0.07	34.3			3.15	-20.4

[a] Solutions are 100 mM sodium chloride, 20 mM sodium cacodylate, and 0.5 mM Na_2EDTA, pH 7. [b] Calculated for 10^{-4} M oligomer concentration.

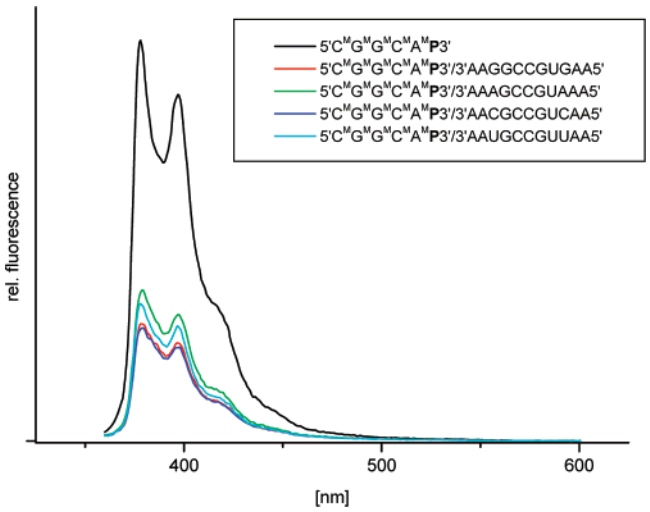

FIGURE 4: Fluorescence at room temperature upon excitation at 340 nm of single stranded 5′*C*^{M}*G*^{M}*G*^{M}*C*^{M}*A*^{M}**P**3′ (black) and duplexes with 3′AAA*GCCGU***A**AA5′ (green), 3′AAU*GCCGU***U**AA5′ (blue), 3′AAG*GCCGU***G**AA5′ (red) and 3′AAC*GCCGU***C**AA5′ (dark blue) RNA oligonucleotides. Italic font marks complementary fragment within the duplexes, whereas bold font marks opposite to pyrene nucleotide. Concentration of each strand was 0.3 μM.

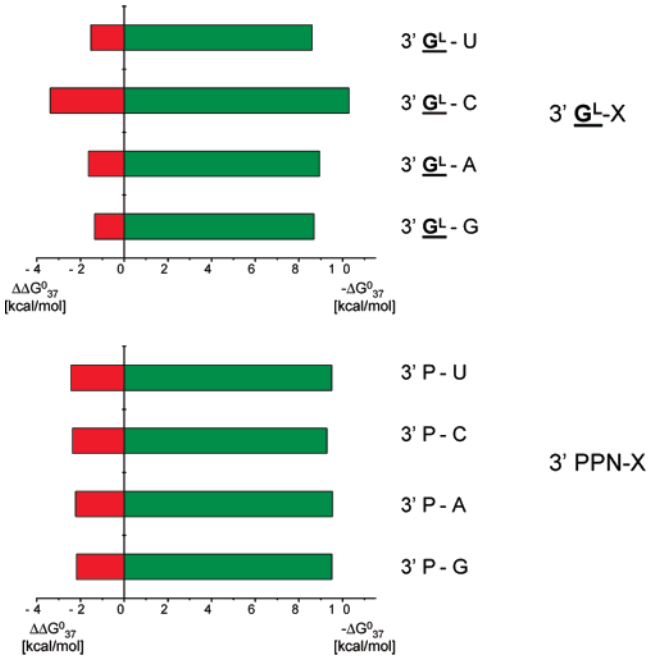

FIGURE 5: Comparison of thermodynamic stability (ΔG°_{37} marked in green) and effects of addition of LNA-G or PPN at 3′-end of 2′-*O*-Me-RNA/RNA duplexes ($\Delta\Delta G^\circ_{37}$ marked in red). For free energy values see Tables 1 and 3.

kcal/mol in comparison with 0.43 kcal/mol in the absence of an additional 3′G^L-G base pair (Table 2). For another

duplex, a 5′-terminal A^M-G mismatch (Figure 3f) decreased stability by 0.88 and 0.32 kcal/mol in the presence and absence of a terminal $3'G^L$-G, respectively (Table 2). Evidently, the presence of 3′-terminal G^L-G or G^L-C base pairs not only increased thermodynamic stability of the hybridization duplexes, but also enhanced discrimination between matched and mismatched 2′-*O*-Me-RNA/RNA duplexes and, in consequence, could improve selectivity of interactions between probes and target RNA. Presumably, similar effects would be seen with G^L-A and G^L-U 3′-terminated 2′-*O*-Me-RNA/RNA duplexes.

As described above, the additional 3′-terminal G^M-X base pairs enhanced thermodynamic stability of 2′-*O*-Me-RNA/RNA duplexes. The improvement, however, was larger for $3'G^{M/L}$-C base pairs than for 3′-terminal mismatches $3'G^{M/L}$-A, $3'G^{M/L}$-U, and $3'G^{M/L}$-G, which complicates interpretation of hybridization experiments.

Thermodynamic analysis of the influence of additional 3′-terminal PPN demonstrated equal enhancement of thermodynamic stability of the 2′-*O*-Me-RNA/RNA duplexes regardless of the nucleotide placed in the opposite strand. Presumably, this is due to stacking of the pyrene ring on the 5′-adjacent helix. The enhancement of duplex stability was −2.17, −2.22, −2.36 and −2.43 kcal/mol for X = G, A, C, and U, respectively (Figure 5, Table 3). This is consistent with thermodynamic studies showing that LNA-pyrene acts as a universal nucleotide (*33*, *34*). Replacement of 5′-adjacent 2′-*O*-methyladenosine by LNA-adenosine caused further stabilization of all duplexes on average by 1.4 kcal/mol, similar to the previously reported data concerning stabilization effects of LNA nucleotides (*15*). Moreover, single mismatches A^M-G placed at 5′-terminal position (Figure 3f) and G^M-U adjacent to PPN (Figure 3g) clearly decreased duplex thermodynamic stability both for the 3′P-G and 3′P-C terminated 2′-*O*-Me-RNA/RNA duplexes (Table 4). As expected, a U^M-C mismatch positioned at the center of a duplex caused the largest destabilization by 2.21 and 3.15 kcal/mol for 3′P-G and 3′P-C terminated duplexes, respectively. Similarly, as discussed earlier, the presence of a 3′-terminal pyrene improved thermodynamic discrimination between matched and mismatched duplexes.

Fluorescence was measured for single stranded $5'C^MG^M$-$G^MC^MA^MP3'$ and its duplexes with complementary 3′AAX*GC*-*CGU*XAA5′ oligoribonucleotides (Figure 4). Fluorescence emission of the 3′-pyrene at 378 and 397 nm decreased by 3- to 4-fold upon binding complementary RNA oligonucleotides. Reduction of fluorescence is basically independent of the nucleotide opposite the pyrene in the duplex. Significant change of fluorescence usually means stacking or intercalating interactions of the pyrene moiety within or on the helix (*17*, *35*, *36*). On the basis of molecular calculations, Christensen and Pedersen (*17*) suggest intercalation of PPN when placed in the middle of the duplex and stacking on the helix when placed at the 5′-terminus. Presumably, placing PPN at the 3′-side of 2′-*O*-MeRNA/RNA duplexes also results in stacking (*32*). Thus PPN provides a built-in fluorescent probe for hybridization in addition to enhancing thermodynamic stability.

It is known that bulged PPN significantly improves thermodynamic stability of DNA duplexes, destabilizes RNA duplexes, and allows discrimination between ssDNA and ssRNA (*17*, *18*, *20*). A 5′-terminal PPN increases the thermodynamic stability of DNA duplexes. It was also shown that PPNs inserted as bulges into 2′-*O*-methyloligoribonucleotides decreased thermodynamic stability of 2′-*O*-Me-RNA/DNA duplexes (*19*). Here, we show strong and equal improvement of 2′-*O*-Me-RNA/RNA duplex thermodynamic stability caused by the presence of PPN at the 3′-terminal position. These features make 3′-PPN a modification of choice for applications of isoenergetic RNA probes.

The thermodynamic data presented here can be applied to design sequence-independent thermodynamic stability of duplexes and enhance the stability of hybridization duplexes between probes and RNA. The same approach could also be used to enhance thermodynamic interactions of duplexes of antisense oligonucleotides, ribozymes or other oligonucleotides with target RNA. Moreover, sliding of complementary oligonucleotides is often observed, particularly for bulged fragments. Application of 3′-pyrene terminated oligonucleotides should avoid shifting of both strands and facilitate formation of only the desired RNA structural motif. That should be useful for NMR, crystallographic and other structural nucleic acid studies. It also has the potential to enhance specificity for nucleic acid based therapeutics.

SUPPORTING INFORMATION AVAILABLE

Tables with complete thermodynamic data. This material is available free of charge via the Internet at http://pubs.acs.org.

REFERENCES

1. Kurreck, J. (2003) Antisense technologies. Improvement through novel chemical modifications, *Eur. J. Biochem. 270*, 1628−1644.
2. Gomez, J., Nadal, A., Sabariegos, R., Beguiristain, N., Martell, M., and Piron, M. (2004) Three properties of the hepatitis C virus RNA genome related to antiviral strategies based on RNA-therapeutics: Variability, structural conformation and tRNA mimicry, *Curr. Pharm. Des. 10*, 3741−3756.
3. Poliseno, L., Mercatanti, A., Citti, L., and Rainaldi, G. (2004) RNA-based drugs: From RNA interference to short interfering RNAs, *Curr. Pharm. Biotechnol. 5*, 361−368.
4. Xia, T. B., SantaLucia, J., Burkard, M. E., Kierzek, R., Schroeder, S. J., Jiao, X. Q., Cox, C., and Turner, D. H. (1998) Thermodynamic parameters for an expanded nearest-neighbor model for formation of RNA duplexes with Watson-Crick base pairs, *Biochemistry 37*, 14719−14735.
5. Mathews, D. H., Sabina, J., Zuker, M., and Turner, D. H. (1999) Expanded sequence dependence of thermodynamic parameters improves prediction of RNA secondary structure, *J. Mol. Biol. 288*, 911−940.
6. Diamond, J. M., Turner, D. H., and Mathews, D. H. (2001) Thermodynamics of three-way multibranch loops in RNA, *Biochemistry 40*, 6971−6981.
7. Mathews, D. H., and Turner, D. H. (2002) Experimentally derived nearest-neighbor parameters for the stability of RNA three- and four-way multibranch loops, *Biochemistry 41*, 869−880.
8. Merino, E. J., Wilkinson, K. A., Coughlan, J. L., and Weeks, K. M. (2005) RNA structure analysis at single nucleotide resolution by selective 2′-hydroxyl acylation and primer extension (SHAPE), *J. Am. Chem. Soc. 127*, 4223−4231.
9. Wilkinson, K. A., Merino, E. J., and Weeks, K. M. (2006) Selective 2′-hydroxyl acylation analyzed by primer extension (SHAPE): quantitative RNA structure analysis at single nucleotide resolution, *Nat. Protoc. 1*, 1610−1616.
10. Mir, K. U., and Southern, E. M. (1999) Determining the influence of structure on hybridization using oligonucleotide arrays, *Nat. Biotechnol. 17*, 788−792.
11. Sohail, M., Akhtar, S., and Southern, E. M. (1999) The folding of large RNAs studied by hybridization to arrays of complementary oligonucleotides, *RNA 5*, 646−655.
12. Southern, E. M., Casegreen, S. C., Elder, J. K., Johnson, M., Mir, K. U., Wang, L., and Williams, J. C. (1994) Arrays of comple-

mentary oligonucleotides for analyzing the hybridization behavior of nucleic-acids, *Nucleic Acids Res. 22*, 1368−1373.
13. Kierzek, E., Kierzek, R., Turner, D. H., and Catrina, I. E. (2006) Facilitating RNA structure prediction with microarrays, *Biochemistry 45*, 581−593.
14. Kierzek, E., Kierzek, R., Moss, W. N., Christensen, S. M., Eickbush, T. H., and Turner, D. H. (2008) Isoenergetic penta- and hexanucleotide microarray probing and chemical mapping provide a secondary structure model for an RNA element orchestrating R2 retrotransposon protein function, *Nucleic Acids Res.*, 10.1093/nar/gkm1085.
15. Kierzek, E., Ciesielska, A., Pasternak, K., Mathews, D. H., Turner, D. H., and Kierzek, R. (2005) The influence of locked nucleic acid residues on the thermodynamic properties of 2′-O-methyl RNA/RNA heteroduplexes, *Nucleic Acids Res. 33*, 5082−5093.
16. Pasternak, A., Kierzek, E., Pasternak, K., Turner, D. H., and Kierzek, R. (2007) A chemical synthesis of LNA-2,6-diaminopurine riboside, and the influence of 2′-O-methyl-2,6-diaminopurine and LNA-2,6-diaminopurine ribosides on the thermodynamic properties of 2′-O-methyl RNA/RNA heteroduplexes, *Nuceic Acids Res. 35*, 4055−4063.
17. Christensen, U. B., and Pedersen, E. B. (2002) Intercalating nucleic acids containing insertions of 1-O-(1-pyrenylmethyl)glycerol: stabilisation of dsDNA and discrimination of DNA over RNA, *Nucleic Acids Res. 30*, 4918−4925.
18. Nielsen, C. B., Petersen, M., Pedersen, E. B., Hansen, P. E., and Christensen, U. B. (2004) NMR structure determination of a modified DNA oligonucleotide containing a new intercalating nucleic acid, *Bioconjugate Chem. 15*, 260−269.
19. Filichev, V. V., Vester, B., Hansen, L. H., and Pedersen, E. B. (2005) Easily denaturing nucleic acids derived from intercalating nucleic acids: thermal stability studies, dual duplex invasion and inhibition of transcription start, *Nucleic Acids Res. 33*, 7129−7137.
20. Christensen, U. B., Wamberg, M., El-Essawy, F. A. G., Ismail, A. E. H., Nielsen, C. B., Filichev, V. V., Jessen, C. H., Petersen, M., and Pedersen, E. B. (2004) Intercalating nucleic acids: The influence of linker length and intercalator type on their duplex stabilities, *Nucleosides, Nucleotides Nucleic Acids 23*, 207−225.
21. Koshkin, A. A., Singh, S. K., Nielsen, P., Rajwanshi, V. K., Kumar, R., Meldgaard, M., Olsen, C. E., and Wengel, J. (1998) LNA (Locked Nucleic Acids): Synthesis of the adenine, cytosine, guanine, 5-methylcytosine, thymine and uracil bicyclonucleoside monomers, oligomerisation, and unprecedented nucleic acid recognition, *Tetrahedron 54*, 3607−3630.
22. Pedersen, D. S., Rosenbohm, C., and Koch, T. (2002) Preparation of LNA phosphoramidites, *Synthesis* 802−808.
23. Koshkin, A. A., Fensholdt, J., Pfundheller, H. M., and Lomholt, C. (2001) A simplified and efficient route to 2′-O, 4′-C-methylene-linked bicyclic ribonucleosides (locked nucleic acid), *J. Org. Chem. 66*, 8504−8512.
24. McBride, L. J., and Caruthers, M. H. (1983) An investigation of several deoxyribonucleoside phosphoramidites useful for synthesizing deoxyoligonucleotides, *Tetrahedron Lett. 24*, 245−248.
25. Kierzek, E., Mathews, D. H., Ciesielska, A., Turner, D. H., and Kierzek, R. (2006) Nearest neighbor parameters for Watson-Crick complementary heteroduplexes formed between 2′-O-methyl RNA and RNA oligonucleotides, *Nucleic Acids Res. 34*, 3609−3614.
26. Borer, P. N. (1975) Optical properties of nucleic acids, absorption and circular dichroism spectra, in *CRC Handbook of Biochemistry and Molecular Biology: Nucleic Acids*, 3rd ed. (Fasman, G. D., Ed.) pp 589−595, CRC Press, Cleveland, OH.
27. Richards, E. G. (1975) Use of tables in calculations of absorption, optical rotatory dispersion and circular dichroism of polyribonucleotides, in *CRC Handbook of Biochemistry and Molecular Biology: Nucleic Acids*, 3rd ed. (Fasman, G. D., Ed.) pp 596−603, CRC Press, Cleveland, OH.
28. McDowell, J. A., and Turner, D. H. (1996) Investigation of the structural basis for thermodynamic stabilities of tandem GU mismatches: Solution structure of $(rGAGGUCUC)_2$ by two-dimensional NMR and simulated annealing, *Biochemistry 35*, 14077−14089.
29. Freier, S. M., Alkema, D., Sinclair, A., Neilson, T., and Turner, D. H. (1985) Contributions of dangling end stacking and terminal base-pair formation to the stabilities of XGGCCp, XCCGGp, XGGCCYp, and XCCGGYp helixes, *Biochemistry 24*, 4533−4539.
30. Freier, S. M., Kierzek, R., Caruthers, M. H., Neilson, T., and Turner, D. H. (1986) Free-energy contributions of G. U and other terminal mismatches to helix stability, *Biochemistry 25*, 3209−3213.
31. Hickey, D. R., and Turner, D. H. (1985) Thermodynamics of duplex formation for ACCGGGp, ACCGGAp, and ACCGGCp, *Biochemistry 24*, 3987−3991.
32. Turner, D. H. (2000), Conformational changes. in *Nucleic acids structures, properties, and functions* (Bloomfield, V. A., Crothers, D. M. and Tinoco, I., Jr.) Chapter 8, pp 259−321, University Science Books, Sausalito, CA.
33. Babu, B. R., Prasad, A. K., Trikha, S., Thorup, N., Parmar, V. S., and Wengel, J. (2002) Conformationally locked aryl C-nucleosides: synthesis of phosphoramidite monomers and incorporation into single-stranded DNA and LNA (locked nucleic acid), *J. Chem. Soc., Perkin Trans. 1* 2509−2519.
34. Babu, B. R., and Wengel, J. (2001) Universal hybridization using LNA (locked nucleic acid) containing a novel pyrene LNA nucleotide monomer, *Chem. Commun.* 2114−2115.
35. Kierzek, R., Li, Y., Turner, D. H., and Bevilacqua, P. C. (1993) 5′-amino pyrene provides a sensitive, nonperturbing fluorescent probe of RNA secondary and tertiary structure formation, *J. Am. Chem. Soc. 115*, 4985−4992.
36. Telser, J., Cruickshank, K. A., Morrison, L. E., and Netzel, T. L. (1989) Synthesis and characterization of DNA oligomers and duplexes containing covalently attached molecular labels: comparison of biotin, fluorescein, and pyrene labels by thermodynamic and optical spectroscopic measurements, *J. Am. Chem. Soc. 111*, 6966−6976.

BI701758Z